Earthquake and Fault Studies by Moment Tensor Inversion and Events Relocation

Lupei Zhu[1]

Dept. Earth and Atmospheric Sciences, SLU, USA

IGCEA, July 1, 2019

[1]Zhu and Helmberger (1996); Zhu and Ben-Zion (2013); Zhu and Zhou (2016); Huang et al. (2018)

Outline

1. Seismic moment tensor inversion for a general seismic source.
2. The Cut-and-Paste (CAP) moment inversion method and gCAP3D.
3. Application of gCAP3D to the 2013 *Ms* 7.0 Lushan earthquake.
4. Seismic and geological evidence of induced earthquakes in TGR.
5. Conclusions.

Moment tensor and the Green's functions

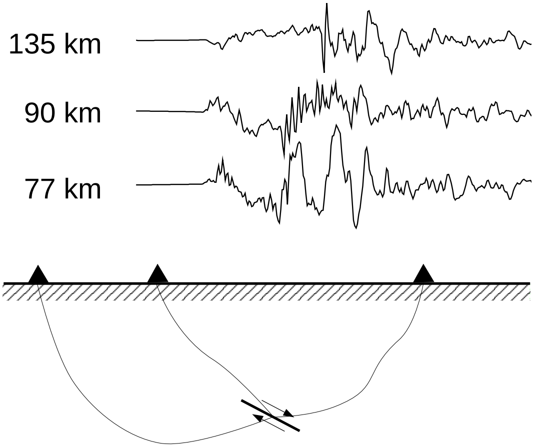

For a DC point seismic source with an impulsive STF,

$$u(t) = M_0 \sum_{i=1}^{3} A_i(\phi, \delta, \lambda) G_i(t), \qquad (1)$$

where $G(t)$'s are Green's functions. For a general point source,

$$u(t) = \sum_{i=1}^{3} \sum_{j=1}^{3} M_{ij} G_{ij}(t), \qquad (2)$$

where **M** is the source moment tensor.

Moment tensor inversion

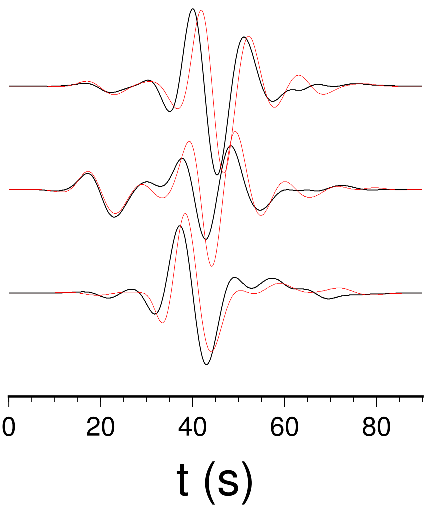

Eq. (2) is a linear function of M_{ij} when the Green's functions are known. But imperfect velocity model and source location/origin time introduce a unknown time shift Δt (Zhao and Helmberger, 1994),

$$u(t) = \sum_{i=1}^{3} \sum_{j=1}^{3} M_{ij} G_{ij}(t - \Delta t), \qquad (3)$$

which makes the moment tensor inversion non-linear.

Parameterization of moment tensor

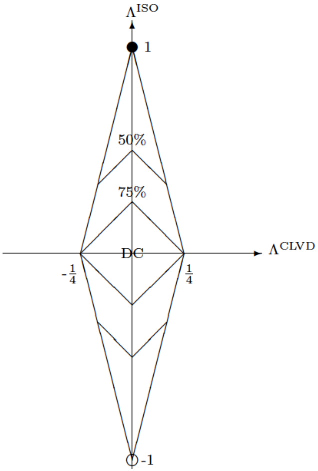

$$M_{ij} = M_0 D_{ij}, \quad (|\mathbf{D}| = \sqrt{2}) \tag{4}$$

$$D_{ij} = \zeta D_{ij}^{\mathrm{ISO}} + \sqrt{1-\zeta^2}\left(\sqrt{1-\chi^2} D_{ij}^{\mathrm{DC}} + \chi D_{ij}^{\mathrm{CLVD}}\right), \tag{5}$$

where

$$D_{ij}^{\mathrm{ISO}} = \sqrt{\frac{2}{3}}\delta_{ij}, \tag{6}$$

$$D_{ij}^{\mathrm{DC}} = n_i v_j + v_i n_j, \tag{7}$$

$$D_{ij}^{\mathrm{CLVD}} = \frac{1}{\sqrt{3}}(2b_i b_j - v_i v_j - n_i n_j), \tag{8}$$

ζ and χ are non-dimensional parameters quantifying the strength of isotropic and CLVD components, respectively (Zhu and Ben-Zion, 2013).

Generalized Cut-and-Paste (gCAP3D) method

gCAP3D (Zhu and Zhou, 2015) uses a grid search to solve Eq. (3) for

$$\mathbf{m} = (\zeta, \chi, \phi, \delta, \lambda)^{\mathrm{T}}. \tag{9}$$

For each possible set of source parameters, it first finds Δt by cross-correlating $u(t)$ and $s(t) = D_{ij} G_{ij}(t)$ and estimates the scalar moment,

$$M_0 = \frac{\|u\|}{\|s\|}. \tag{10}$$

It then calculates the waveform misfit e using the L_2 norm of the difference between observed and predicted waveform,

$$E = \sum_{i=1}^{N_s} \left(w^2 \left(\frac{r_i}{r_0}\right)^2 \left(e_i^{PnlZ} + e_i^{PnlR}\right) + \frac{r_i}{r_0} \left(e_i^{RaylZ} + e_i^{RaylR} + e_i^{Love}\right) \right), \tag{11}$$

$$e = \|u(t) - M_0 s(t - \Delta t)\|^2. \tag{12}$$

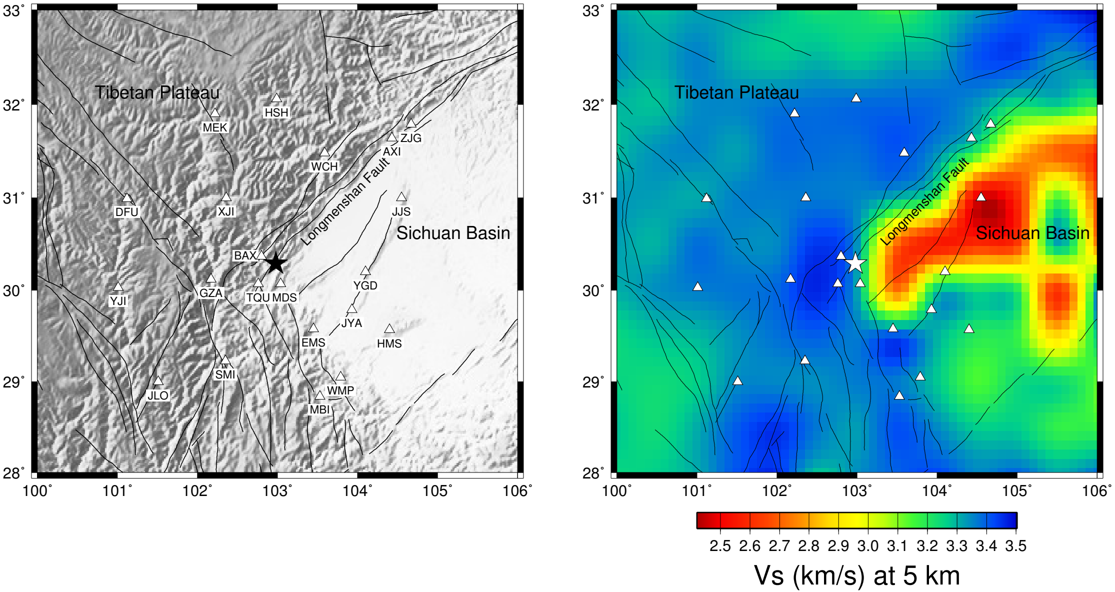

Tibetan Plateau
Sichuan Basin
Longmenshan Fault
HSH
MEK
ZJG
AXI
WCH
DFU
XJI
JJS
BAX
GZA
TQU
MDS
YGD
YJI
JYA
EMS
HMS
SMI
JLO
WMP
MBI
33°
32°
31°
30°
29°
28°
100°
101°
102°
103°
104°
105°
106°
2.5
2.6
2.7
2.8
2.9
3.0
3.1
3.2
3.3
3.4
3.5
Vs (km/s) at 5 km

Unit Cell for Staggered-Grid Formulation

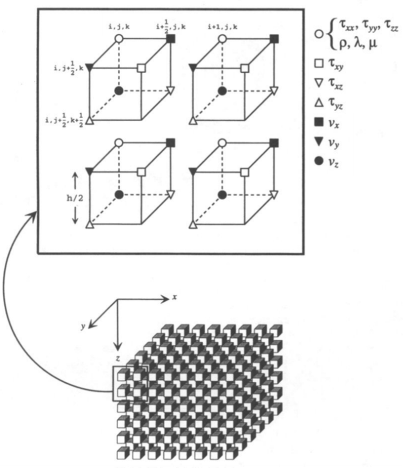

- EMOD3D code by R. Graves (1996).
- Staggered grid, 4th-order FD.
- 450×450×150 km.
- Grid spacing 1 km, f_{max}=0.4 Hz.
- Use the reciprocity principle to reduce the number of FD runs.
- Takes ∼4 Hrs. per station.

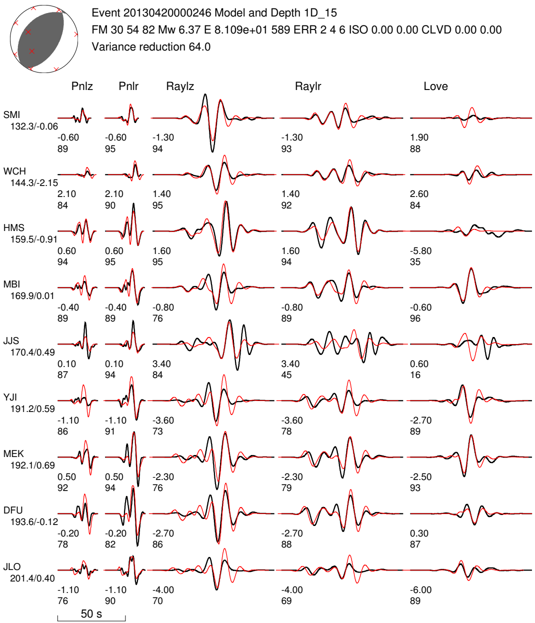
Event 20130420000246 Model and Depth 1D_15
FM 30 54 82 Mw 6.37 E 8.109e+01 589 ERR 2 4 6 ISO 0.00 0.00 CLVD 0.00 0.00
Variance reduction 64.0
Pnlz
Pnlr
Raylz
Raylr
Love
SMI 132.3/-0.06
-0.60 89
-0.60 95
-1.30 94
-1.30 93
1.90 88
WCH 144.3/-2.15
2.10 84
2.10 90
1.40 95
1.40 92
2.60 84
HMS 159.5/-0.91
0.60 94
0.60 95
1.60 95
1.60 94
-5.80 35
MBI 169.9/0.01
-0.40 89
-0.40 89
-0.80 76
-0.80 89
-0.60 96
JJS 170.4/0.49
0.10 87
0.10 94
3.40 84
3.40 45
0.60 16
YJI 191.2/0.59
-1.10 86
-1.10 91
-3.60 73
-3.60 78
-2.70 89
MEK 192.1/0.69
0.50 92
0.50 94
-2.30 76
-2.30 79
-2.50 93
DFU 193.6/-0.12
-0.20 78
-0.20 82
-2.70 86
-2.70 88
0.30 87
JLO 201.4/0.40
-1.10 76
-1.10 90
-4.00 70
-4.00 69
-6.00 89
50 s

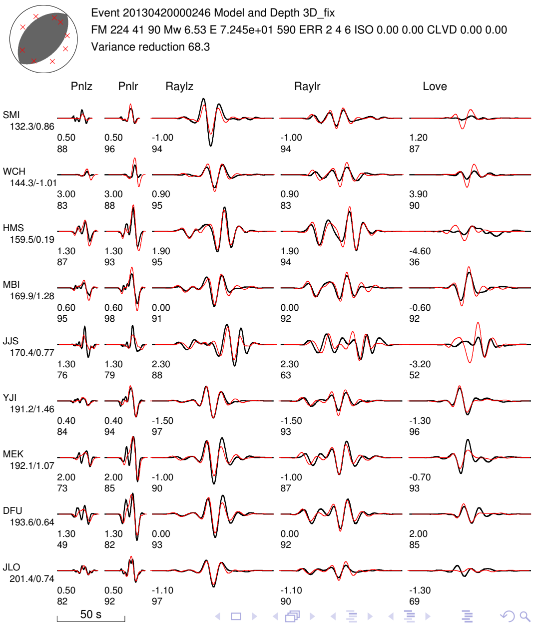
Event 20130420000246 Model and Depth 3D_fix
FM 224 41 90 Mw 6.53 E 7.245e+01 590 ERR 2 4 6 ISO 0.00 0.00 CLVD 0.00 0.00
Variance reduction 68.3
Pnlz
Pnlr
Raylz
Raylr
Love
SMI 132.3/0.86
0.50 88
0.50 96
-1.00 94
-1.00 94
1.20 87
WCH 144.3/-1.01
3.00 83
3.00 88
0.90 95
0.90 83
3.90 90
HMS 159.5/0.19
1.30 87
1.30 93
1.90 95
1.90 94
-4.60 36
MBI 169.9/1.28
0.60 95
0.60 98
0.00 91
0.00 92
-0.60 92
JJS 170.4/0.77
1.30 76
1.30 79
2.30 88
2.30 63
-3.20 52
YJI 191.2/1.46
0.40 84
0.40 94
-1.50 97
-1.50 93
-1.30 96
MEK 192.1/1.07
2.00 73
2.00 85
-1.00 90
-1.00 87
-0.70 93
DFU 193.6/0.64
1.30 49
1.30 82
0.00 93
0.00 92
2.00 85
JLO 201.4/0.74
0.50 82
0.50 92
-1.10 97
-1.10 90
-1.30 69
50 s

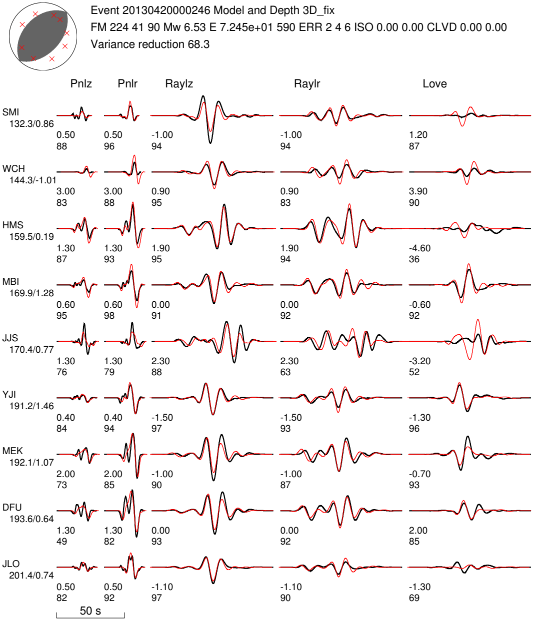
Event 20130420000246 Model and Depth 3D_fix
FM 224 41 90 Mw 6.53 E 7.245e+01 590 ERR 2 4 6 ISO 0.00 0.00 CLVD 0.00 0.00
Variance reduction 68.3
Pnlz
Pnlr
Raylz
Raylr
Love
SMI
132.3/0.86
0.50 88
0.50 96
-1.00 94
-1.00 94
1.20 87
WCH
144.3/-1.01
3.00 83
3.00 88
0.90 95
0.90 83
3.90 90
HMS
159.5/0.19
1.30 87
1.30 93
1.90 95
1.90 94
-4.60 36
MBI
169.9/1.28
0.60 95
0.60 98
0.00 91
0.00 92
-0.60 92
JJS
170.4/0.77
1.30 76
1.30 79
2.30 88
2.30 63
-3.20 52
YJI
191.2/1.46
0.40 84
0.40 94
-1.50 97
-1.50 93
-1.30 96
MEK
192.1/1.07
2.00 73
2.00 85
-1.00 90
-1.00 87
-0.70 93
DFU
193.6/0.64
1.30 49
1.30 82
0.00 93
0.00 92
2.00 85
JLO
201.4/0.74
0.50 82
0.50 92
-1.10 97
-1.10 90
-1.30 69
50 s

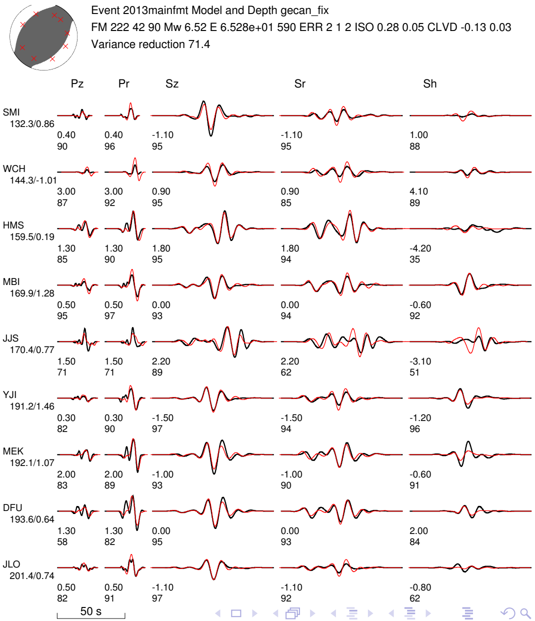
Event 2013mainfmt Model and Depth gecan_fix
FM 222 42 90 Mw 6.52 E 6.528e+01 590 ERR 2 1 2 ISO 0.28 0.05 CLVD -0.13 0.03
Variance reduction 71.4
Pz
Pr
Sz
Sr
Sh
SMI
132.3/0.86
0.40 90
0.40 96
-1.10 95
-1.10 95
1.00 88
WCH
144.3/-1.01
3.00 87
3.00 92
0.90 95
0.90 85
4.10 89
HMS
159.5/0.19
1.30 85
1.30 90
1.80 95
1.80 94
-4.20 35
MBI
169.9/1.28
0.50 95
0.50 97
0.00 93
0.00 94
-0.60 92
JJS
170.4/0.77
1.50 71
1.50 71
2.20 89
2.20 62
-3.10 51
YJI
191.2/1.46
0.30 82
0.30 90
-1.50 97
-1.50 94
-1.20 96
MEK
192.1/1.07
2.00 83
2.00 89
-1.00 93
-1.00 90
-0.60 91
DFU
193.6/0.64
1.30 58
1.30 82
0.00 95
0.00 93
2.00 84
JLO
201.4/0.74
0.50 82
0.50 91
-1.10 97
-1.10 92
-0.80 62
50 s

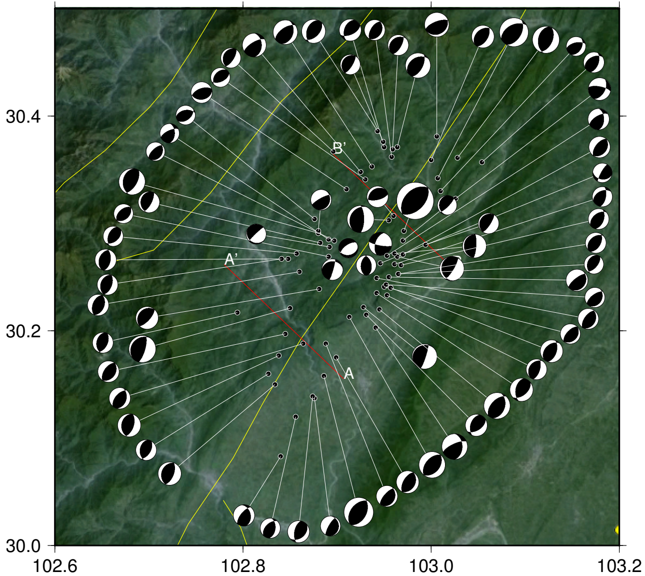

B'
A'
A
30.4
30.2
30.0
102.6
102.8
103.0
103.2

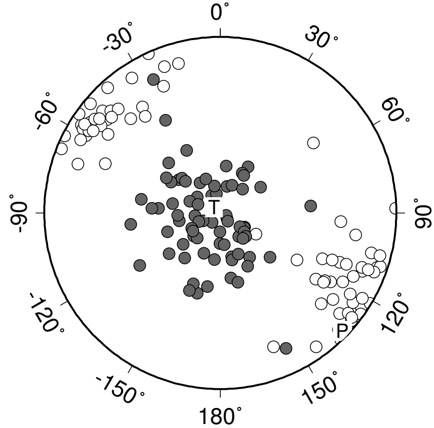

0°
30°
60°
90°
120°
150°
180°
-150°
-120°
-90°
-60°
-30°
T
P

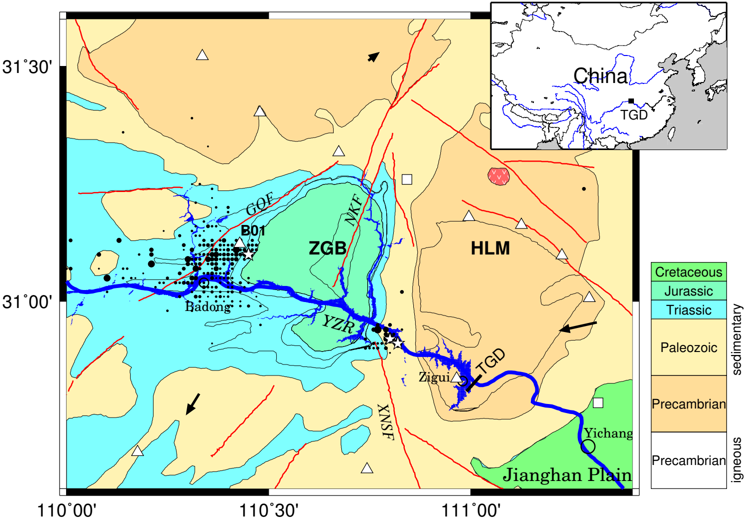
31˚30'
31˚00'
110˚00'
110˚30'
111˚00'
China
TGD
GOF
NKF
B01
ZGB
HLM
Badong
YZR
TGD
Zigui
XNSF
Yichang
Jianghan Plain
Cretaceous
Jurassic
Triassic
Paleozoic
Precambrian
sedimentary
Precambrian
igneous

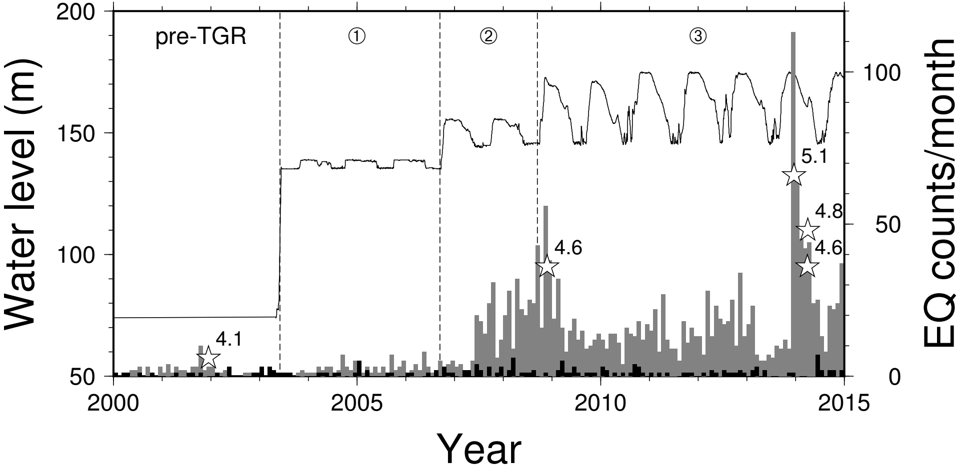

pre-TGR
①
②
③
Water level (m)
200
150
100
50
EQ counts/month
100
50
0
4.1
4.6
5.1
4.8
4.6
2000
2005
2010
2015
Year

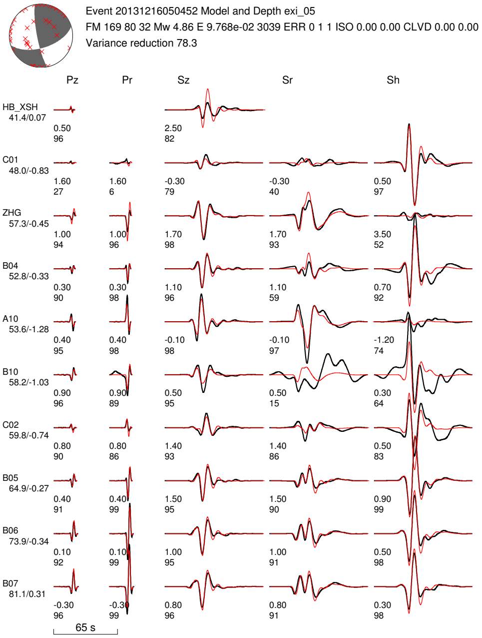
Event 20131216050452 Model and Depth exi_05
FM 169 80 32 Mw 4.86 E 9.768e-02 3039 ERR 0 1 1 ISO 0.00 0.00 CLVD 0.00 0.00
Variance reduction 78.3
Pz
Pr
Sz
Sr
Sh
HB_XSH 41.4/0.07
C01 48.0/-0.83
ZHG 57.3/-0.45
B04 52.8/-0.33
A10 53.6/-1.28
B10 58.2/-1.03
C02 59.8/-0.74
B05 64.9/-0.27
B06 73.9/-0.34
B07 81.1/0.31
65 s

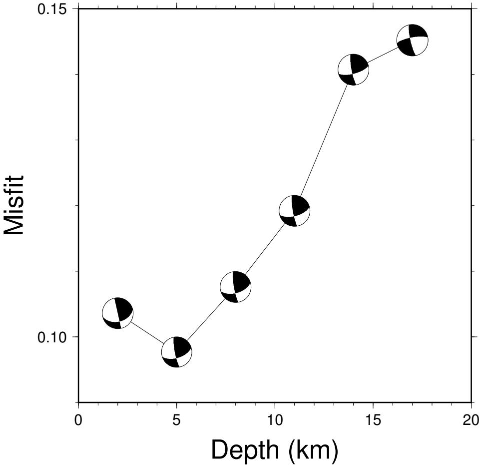
0.15
0.10
Misfit
0
5
10
15
20
Depth (km)

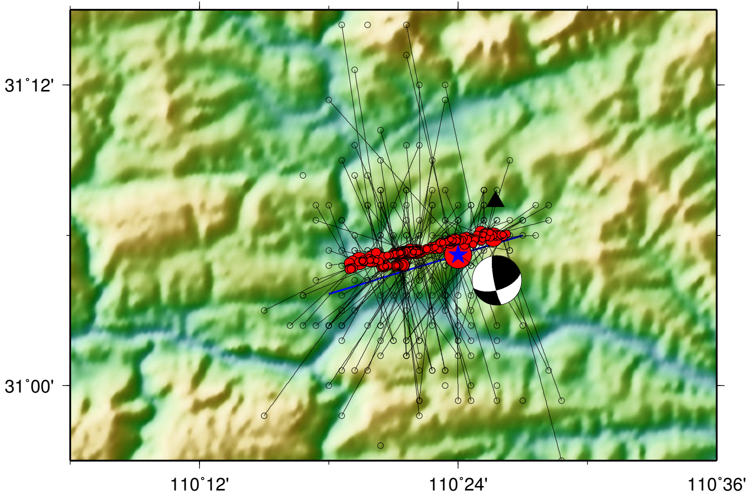

Out of 219 events with 20 km of the mainshock, 205 were relocated along a line in N73°.

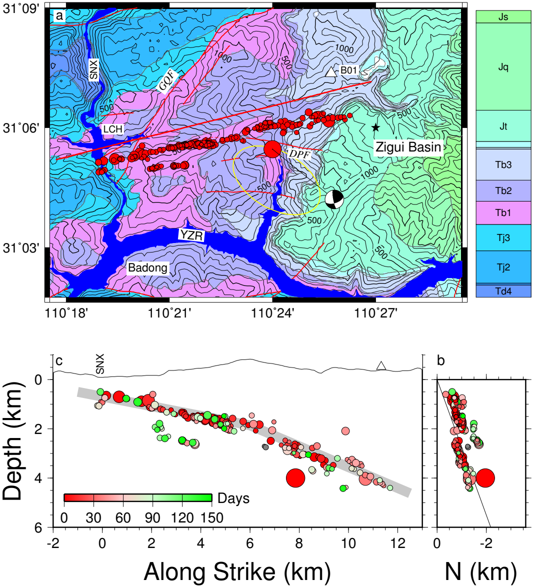

a
31°09'
31°06'
31°03'
110°18'
110°21'
110°24'
110°27'
SNX
GQF
LCH
B01
DPF
Zigui Basin
YZR
Badong
1000
500
Js
Jq
Jt
Tb3
Tb2
Tb1
Tj3
Tj2
Td4
c
b
Depth (km)
Along Strike (km)
N (km)
Days
0 30 60 90 120 150

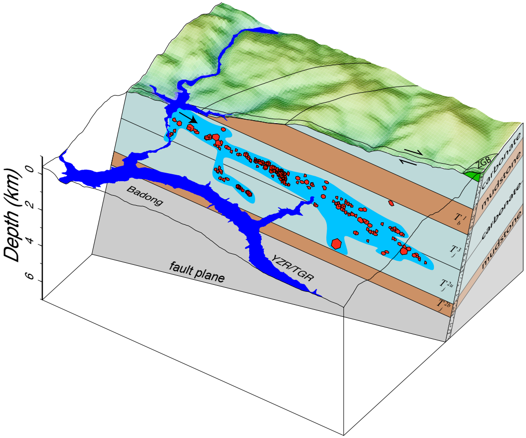

Depth (km)
0
2
4
6
Badong
fault plane
YZR/TGR
ZGB
carbonate
mudstone
carbonate
mudstone

Conclusions

1. We developed a method for determining moment tensors using 3D velocity models.
2. The method has been fully automated for real-time moment tensor inversion.
3. We applied the method to the 2013 Ms 7.0 Lushan earthquake sequence and obtained 75 moment tensor solutions ranging from Mw 6.5 to 3.4. The mainshock is a reverse faulting on a plane dipping 40-47°to NW.
4. We also applied the method and HypoDD to the 2013 M 5.1 Badong earthquake sequence in the Three Gorges Reservoir. We found an unmapped fault of $\sim$15 km long that is seismically active and has potential to produce a large earthquake of $M >$6.5. The results suggest that the sequence was induced by water infilteration in a fractured carbonate rock formation from the reservoir.